

SOL density variations during ICRF heating and gas injection

V. Petrzilka¹, M. Goniche², G. Corrigan³, J. Ongena⁴, V. Bobkov⁵, L. Colas², A. Ekedahl²,
P. Jacquet³, M.-L. Mayoral³, and JET EFDA contributors^{*}

JET-EFDA, Culham Science Centre, OX14 3DB, Abingdon, UK

¹Association EURATOM-IPP.CR, Za Slovankou 3, 182 21 Praha 8, Czech Republic

²CEA, IRFM, F-13108 Saint-Paul-lez-Durance, France

³Euratom/CCFE Fusion Association, Culham Science Centre, Abingdon, OX14 3DB, UK

⁴Association Euratom-Belgian State, ERM-KMS, B-1000 Brussels, Belgium

⁵Max-Planck-Institut für Plasmaphysik, EURATOM Association, Garching, Germany

In this paper, we present modeling results of the effect of gas injection on the SOL (Scrape-off-layer) density profiles (n_{eSOL}) during ICRF (Ion Cyclotron Resonance Frequency) heating. Gas injection during ICRF has been tested in several tokamaks with the goal of improving the coupling by modifying the density profile in front of the antenna, thus facilitating the fast wave propagation through the evanescent layer [1-4].

The EDGE2D / NIMBUS code was adapted to model the presence of a wide SOL and a magnetic geometry with a 2nd X-point near to the top of the wall (as in JET pulses #68109-13 [3,5]). In contrast to the computational grid for the configurations considered in [6] that have a SOL width of about 10 cm at the Outer Mid-Plane (OMP), EDGE2D simulations with the 2nd X point at the top are only carried out considering about 4 cm of SOL in the OMP. This is because the EDGE2D computational grid is restricted to a rather narrow OMP SOL layer in these ITER relevant configurations. One possibility is then to continue into the far SOL with "ad hoc" assumptions about transport with essentially 1D model. This then prohibits the modeling distant from the separatrix using EDGE2D. Following previous work [7], we have attempted to overcome this problem and to maintain the modeled SOL width at about 10 cm by introducing a limiter (particle sink) protruding radially down from the top. Then, the locations radially near the antenna front face are connected to the wall, similarly to the above mentioned ITER-like configuration with a 2nd X-point at the top. In the modeled 2D geometry discussed in this paper, the gas puff location is by definition magnetically connected to the ICRF antenna location. We assume that the ICRF wave does not contribute to ionization of the neutral gas by local SOL RF energy absorption/heating. The SOL ionization and related n_{eSOL} increase are due to increased SOL temperature, similarly as during any core heating. The power crossing the separatrix from the core to the SOL was set to 10 MW plus ICRF power from 0 to 3 MW. It is known that the SOL diffusion coefficient significantly varies with the SOL plasma temperature and density [8], themselves varying with the gas puff. Therefore, we

* See the Appendix of F. Romanelli et al., Proceedings of the 23rd IAEA Fusion Energy Conference 2010, Daejeon, Korea

considered several values of the diffusion coefficient D and heat diffusivities in the simulations, similarly as in [6]. The particle (and heat) diffusion coefficients were set to constant $0.1 \text{ m}^2/\text{s}$ value from the core to the separatrix and to either the same value of $0.1 \text{ m}^2/\text{s}$ also in the SOL (case a) or to various constant values up to $2 \text{ m}^2/\text{s}$ in the SOL (case b). Fig. 1 compares $n_{e\text{SOL}}$ for OMP and top gas injection for case a and shows well the lower efficiency of the top gas injection compared to the OMP one. This difference is similar for all values of D considered in the computations.

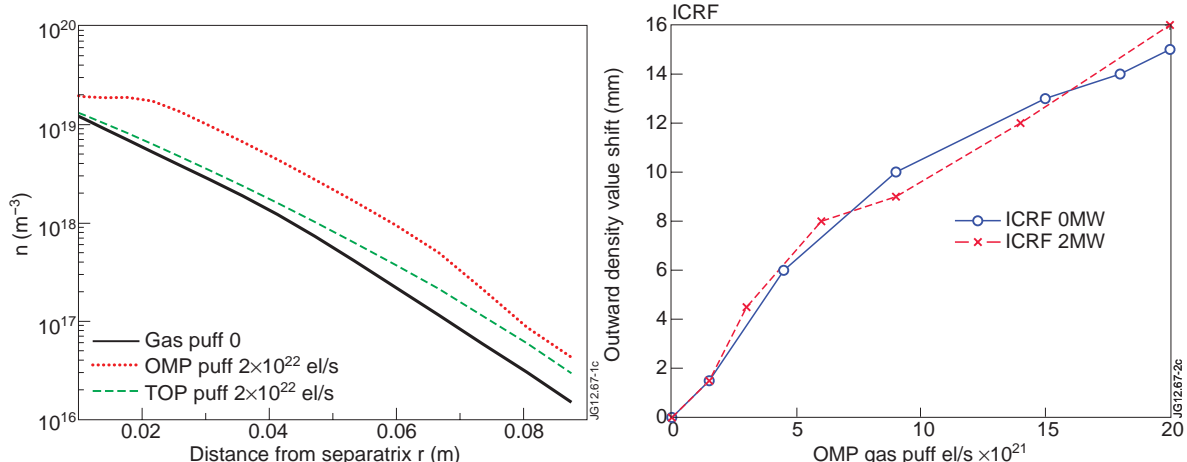


Fig. 1 (left). OMP $n_{e\text{SOL}}$ profiles, TOP and OMP gas puff $2 \times 10^{22} \text{ el/s}$ and ICRF power level of 2 MW. Fig. 2 (right). Outward OMP shift of the cut-off density value of $2 \times 10^{18} \text{ m}^{-3}$. (JET scenarios [3]) for different OMP gas injection levels.

The computed OMP outward shift of the FW cut-off density for JET scenarios described in [3] ($2 \times 10^{18} \text{ m}^{-3}$), as a function of the gas puff, is shown in Fig. 2 for zero ICRF power (blue) and for 2MW of ICRF power (red). It can be seen that the density shift depends on the additional power only marginally, in agreement with [2]. We also compared simulated $n_{e\text{SOL}}$ profiles with experimental ones from RCP (Reciprocating Probe) and Li-beam measurements for JET shots #68111-68113 that had various gas injection rates from different locations [3]: - #68111: no gas injected from the OMP (Gas Injection Module GIM 6), $1 \times 10^{22} \text{ el/s}$ injected from the divertor (GIM9 and GIM10); - #68112 : $4 \times 10^{21} \text{ el/s}$ gas injected from GIM6, $1 \times 10^{22} \text{ el/s}$ injected from GIM9 and GIM10; - JET pulse #68113: no additional gas injected. For case a) D profile, the comparison with experiments was rather poor, and we do not show it in figures. Fig. 3 shows comparison of the simulations for case b) profiles with $D=1 \text{ m}^2/\text{s}$ further out in the SOL. However, a reasonable fit of the simulation results with experimental data was obtained only after enlarging twice the radial scale when plotting the modeling results. This can be explained as follows: According to [8], it is often observed on JET that the density radial variation in the SOL follows an exponential decay. From a simple diffusion model, $\lambda_n \approx (D L/c_s)^{1/2}$ where c_s is the acoustic speed, and L is the connection length. The enlargement of the radial scale in Fig. 3 can be therefore considered as a corresponding enlargement of the diffusion coefficient D **and** of the SOL width. In simulations shown in Fig. 3, we did not use

divertor gas injection, only top and OMP gas injection. As can be seen, top and OMP gas injection is approximately of the same efficiency for the n_{eSOL} enhancement in the RCP/Li-beam location. The OMP gas injection is more efficient

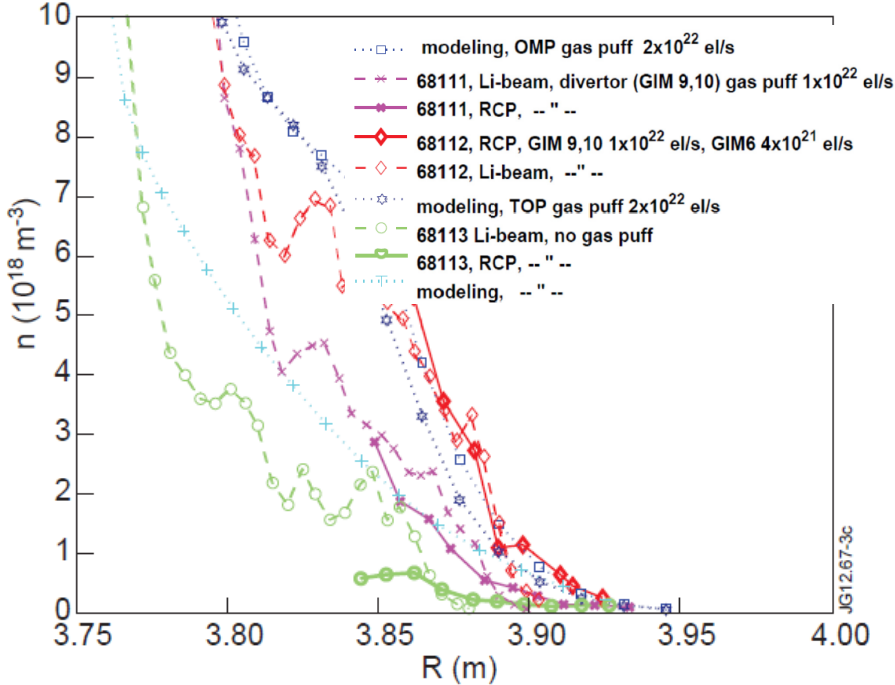


Fig. 3. Comparison of n_{eSOL} profiles simulations at the RCP and Li beam locations with the JET experimental profiles using $D=1 \text{ m}^2/\text{s}$. The RCP and Li beam measurements were done at 8 s, at ROG 14 cm.

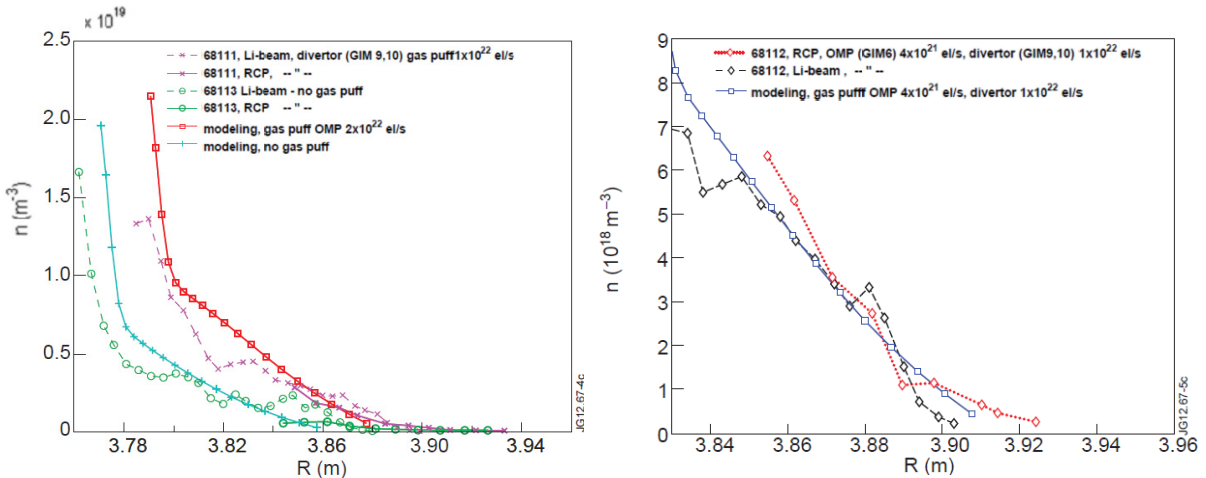


Fig. 4 (left). Comparison of n_{eSOL} profiles simulations at the RCP and Li beam locations with the JET experimental profiles using $D=1.75 \text{ m}^2/\text{s}$. For the red modeling curve, the modeling separatrix is at $R=3.79 \text{ m}$. Fig. 5 (right). Comparison of n_{eSOL} profiles simulations at the RCP and Li beam locations with the experimental profiles from pulse 68112 using $D=1.75 \text{ m}^2/\text{s}$ and using the same gas puff as in the experiment. The modeling separatrix is at the coordinate $R=3.82 \text{ m}$.

for OMP n_{eSOL} enhancement also in this case, similarly as is also shown in Fig. 1. For a still better fit to experimental data, we further enlarged D in the modeling to $1.75 \text{ m}^2/\text{s}$ further out in the SOL, cf. Fig. 4. The divertor puff in simulations gives more precise fit of simulations to experiments in far SOL, as shows next Fig. 5. This figure contains

comparison of modeling with shot #68112 data, for the same gas puff rates and locations in simulations as were that used in the experiment. Note that the top gas puff lower efficiency for OMP n_{eSOL} enhancement compared to the OMP puff, is nevertheless untrue if one looks at the n_{eSOL} at the RCP or Li beam locations (see blue squares and stars on Fig. 3), which are more near to the gas puff location at the top of the wall. We also note that the computed profiles are radially shifted to the right by about 2.5 cm in order to fit the simulations as well as possible to the RCP and Li-beam data in the far SOL. The exception is the profile without the puff (#68113), where the computed profile is shifted by 1 cm only. The shift was needed because the modeled SOL width of 9 cm is smaller than the radial outer gap (ROG =14 cm at the RCP – Li beam measurement time 8 s) in the experiments. Even if the best fit to experiments is found for the largest diffusion coefficient D (Fig. 5), we think that it is useful to show also the trends with varying D value, and therefore to show the results for lower D values in the other figures: D can vary in various experimental conditions. To conclude, the modeling results for OMP gas puff are for larger values of D in SOL not far from the experimental results, as is seen in Figs. 3, 4 and 5. To our opinion, the modeling and experiments do not indicate that a significant direct SOL ionization by ICRF wave takes place in experiments, in contrast to the case of the lower hybrid (LH) heating [3,4]. With significant direct SOL ionization in the experiments, like at LH heating, the modeled and measured profiles typically exhibit strong local n_{eSOL} enhancement, even a density bump [6, 7]. Let us note that for the case of LH wave launching, only introduction of enhanced ionization [6] was successful for fitting the data to the modeling curves [3,4,7]. Observations from ASDEX-U [4] by Li-beam and interferometry exhibit similar n_{eSOL} increase and outward shifts of the cut-off density as that found in simulations at similar gas puff rates. In agreement with some observations [2], the OMP gas puff is in the simulations more efficient for the OMP density enhancement (Figs. 1,2) than the TOP gas puff. Therefore, the OMP gas puff location should be preferred also in experiments for the purpose of OMP n_{eSOL} enhancement. The gas puff rate is needed a bit higher in simulations than it is in the experiments. The reason might be that it is not possible in the 2D model used to include effects of the distance between the gas puff location and the antenna on the density profile in front of the antenna, while experiments show that the smaller is this distance, the larger is the beneficial effect on the antenna loading [1, 2].

This work was supported by EURATOM and carried out within the framework of the European Fusion Development Agreement. The views and opinions expressed herein do not necessarily reflect those of the European Commission. V. P. acknowledges support of the Czech Science Foundation Grant 205/10/2055, and of MSMT CR Grant LG11018.

- [1] M.-L. Mayoral et al., 23rd IAEA Conference 2010, Daejeon, Korea, paper ITR/P1-11.
- [2] R. I. Pinsker et al., paper O4.124, 37th EPS Conference 2010.
- [3] M.-L. Mayoral et al., 17th Topical Conf. on RF power in Plasmas, AIP Conf. Proc. 933 (2007), p55.
- [4] P. Jacquet et al., Nuclear Fusion 52 (2012) 042002.
- [5] V. Petrzilka et al., 38th EPS Conf. 2011. P4.099; A. Ekedahl et al., PPCF 54 (2012) 074004.
- [6] M. Goniche et al., Plasma Phys. Control. Fusion 51 (2009) 044002.
- [7] V. Petrzilka et al.: paper P4.207, 36th EPS Conf. 2009; Plasma Phys. Control. Fusion 54 (2012) 074005.
- [8] P. C. Stangeby et al., Plasma Physics and Controlled Fusion, 32. (1990) 475.